Desalination and Water Treatment
www.deswater.com

doi:10.5004/dwt.2019.24566

165 (2019) 290–300
October

Effect of synthesis parameters on the formation 4A zeolite crystals: characterization analysis and heavy metals uptake performance study for water treatment

Sama M. Al-Jubouri[a,*], Huda Adil Sabbar[b], Hamzah A. Lafta, Basma I. Waisi[a]

[a]*Department of Chemical Engineering, College of Engineering, University of Baghdad, Aljadria, Baghdad, P.O. Box: 47024, Iraq, email: sama.al-jubouri@coeng.uobaghdad.edu.iq (S.M. Al-Jubouri), basmawaisi@coeng.uobaghdad.edu.iq (B.I. Waisi),*
[b]*Biological Engineering Chemical, Al-Khwarizmi College of Engineering, University of Baghdad, Aljadria, Baghdad, Iraq, email: enghudaadil@gmail.com (H.A. Sabbar), hamzaabdalameer75@gmail.com (H.A. Lafta)*

Received 15 March 2019; Accepted 12 June 2019

ABSTRACT

This paper sheds light on key factors controlling the growth of 4A zeolite crystals during a conventional hydrothermal synthesis. SiO_2/Al_2O_3 ratio, Na_2O/SiO_2 ratio, H_2O/Na_2O ratio, crystallization time and crystallization temperature affecting zeolite growth during the hydrothermal synthesis were investigated. Optimizing the SiO_2/Al_2O_3 ratio, Na_2O/SiO_2 ratio and H_2O/Na_2O ratio crucially controls the formation of pure zeolite. It was found that mild alkalinity favors crystallization of 4A zeolite. Also for a chosen gel formula, crystallization temperature and time significantly affect the morphology and crystal size of the final products. Conducting the crystallization at 100°C for 4 h produced crystals having cubic morphology with planar surfaces, well-defined and sharp edges. Rietveld refinement analysis was used to study the influence of crystallization temperature on the structure of 4A zeolite. The micro strain values for an amorphous sample significantly varied from those values for the well-crystallized samples. Also, the efficacy of the prepared 4A zeolite for heavy metal removal was examined with both nickel and lead ions. All 4A zeolite samples showed significant heavy metal uptakes due to obtaining a well-crystallized structure which offers sufficient surface area for ion-exchange. Removal of lead ion encompasses both ion-exchange and precipitation process simultaneously.

Keywords: 4A zeolite; Hydrothermal synthesis; Characterization; Ion-exchange; Nickel; Lead

1. Introduction

Disposal of wastewater containing heavy metals into the environment continuously increases as a result of rapid industrialization and economic development [1]. Electroplating industry, metallurgical industry, chemical manufacturing, battery manufacturing and tannery operations are realistic examples of industrial applications that release heavy metal [2]. In addition, some heavy metals are naturally occurring elements such as copper, lead, zinc, cobalt and nickel [3]. Heavy metals are stable and persistent toxic pollutants to aquatic ecosystem [4]. Discharging of industrial waste holding many toxic heavy metals to the environment leads to serious soil and water pollution [5]. These elements can accumulate in aquatic organisms and consequently affect human health by causing numerous diseases and disorders when exceeding specific levels [6]. Low concentrations of heavy metals are necessary for our health; however, large amounts of these elements may cause acute or chronic toxicity [3].

Nickel is a more recalcitrant pollutant in comparison with other heavy metals; it is commonly used in various industries, thus its removal from waste waters receives greater attention [6]. Lead enters the ecosystem through the soil, air and water; accordingly, its harmful effect on human health clearly appears in damaging enzyme function, muscles, nervous system and other organs [7,8]. Therefore, the World

*Corresponding author.

Health Organization (WHO) set 0.07 ppm as an acceptable concentration of nickel in drinking water [9]; while 0.02 ppm of nickel in drinking water was set by European Union (EU) [10]. Also, both WHO and EU set 0.01 ppm as an acceptable concentration for lead in drinking water [9,10].

The global awareness of the environmental deterioration has been giving unlimited importance to wastewater treatment over the years. This requires developing various treatment techniques compatible with wastewater characteristics; especially when containing high concentrations of toxic metals [2] (even up to 500 ppm [11]). Developing of new treatment methods based on inexpensive raw materials and effective pollutant removal is demanded to optimize the wastewater treatment method [5]. Numerous different treatment methods has been used for dissolved metal removal such as ultra filtration, reverse osmosis, electro dialysis, electrolysis, solvent extraction, evaporation, chemical precipitation, coagulation–precipitation, adsorption and ion-exchange [1–3].

Among various methods used for heavy metals removal, adsorption and ion-exchange are commonly effective processes especially when low-cost materials used for the removal process [2]. Great attention has been paid to the ion-exchange process because it encompasses convenient operations, shows efficient removal even of low concentrations of contaminants and exhibits selectivity to remove heavy metals [12]. Many different materials have been studied for this goal including polymeric resins, natural and synthetic zeolites [3,13]. Zeolites are well-recognized effective ion-exchangers/adsorbents that can easily and selectively uptake metal cations having positive charges in their framework to leave less sludge amount and commit to the hard regulations of waste disposal [3,6].

Zeolites are micro porous aluminosilicate minerals with a crystalline structure consisting of AlO_4 and SiO_4 tetrahedrons joined together by shared oxygen atoms to form different open porous structures with different characteristics and properties [14]. Incorporation of Al into the silica framework results in a negatively charged framework which requires the presence of non-framework cations within the structure to neutralize the charge [15,16]. Water molecules can be reversibly evacuated from zeolite's structure by drying. Also, the cations are mobile and generally undergo ion-exchange [17]. Typically, zeolites have a pore diameter in the range of 0.3–1 nm [18] and these micro pores and voids make up to 50% of the zeolite crystal volume [19].

4A Zeolite, which is called 4A zeolite, NaA zeolite or Linde type A (zeolite LTA), is one of the most common synthesized zeolites has a low silica to aluminum ratio. NaA Zeolite has a pore size of 0.4 nm which allows possible separation of small molecules according to the size variation. The pore size of NaA can be changed to 0.5 nm or 0.3 nm when sodium is exchanged with calcium or potassium respectively [20,21]. NaA zeolite has Si/Al molar ratio of 1, therefore it contains high cation concentration and large exchange capacities [22]. The morphology and crystal size distribution of zeolite have a significant effect on their properties and applications because the physical and chemical properties of zeolites largely depend on their structures [14,23]. NaA zeolite was first synthesized by a hydrothermal method and has been extensively used for different industries as zeolite membranes, catalysts, ion exchangers and adsorbents [14].

The economic importance of zeolites promotes scientists to serious work in zeolite characterization to understand the structures and formation of zeolites and create a relationship between the structure and properties [24]. Synthesis techniques offer flexibility in directing zeolite topology, cation type in the framework and pore size [23]. However, synthesis of zeolites from chemical sources is expensive, it produces materials with high-purity, precisely engineered chemical and desired physical properties [22]. The hydrothermal method is the most common among several synthesis methods, so far. The hydrothermal synthesis is a multiphase reaction-crystallization technique, involves both amorphous and crystalline solid phases and at least one liquid phase [24].

Understanding the anisotropic properties of a material essentially depends on the texture analysis which generally uses either X-ray or neutron diffraction data that offer very effective means for texture analysis [25]. Rietveld method performed by materials analysis using diffraction (MAUD) software has been applied to neutron diffraction and then applied to X-ray diffraction data for texture analysis purpose [26,27]. Rietveld refinement method uses models that deals with the anisotropic broadening of the diffracted peaks produced by crystallite size and micro strain [28]. The refinement of the anisotropic width parameters related to these models is achieved to enhance the fitting and improve the refinement of the atomic crystal structure. The quantitative analysis resulting from Rietveld refinement must be considered to retrieve the micro structural information contained therein. In some cases, the results obtained help to understand the intrinsic properties of the crystalline material under the investigation [29]. Popa model is a common approach compatible with the Rietveld refinement method which allows calculating of crystal size and micro strain for anisotropic crystal [28].

Generally, zeolite synthesis by a hydrothermal technique is influenced by batch composition, Si/Al ratio, the solvent, alkalinity, inorganic cations, organic templates, aging, seeding, stirring, crystallization temperature and crystallization time [14,30]. In this contribution, the influence of SiO_2/Al_2O_3 molar ratio (1, 2, 2.2), Na_2O/SiO_2 molar ratio (2.29, 2.5, 3), H_2O/Na_2O molar ratio (35, 45, 60), crystallization temperature and time on the crystallization of 4A zeolite was studied in term of the structure and morphology of 4A zeolite produced. Also, the uptake property of 4A zeolite samples with respect to nickel and lead ions was studied.

2. Experimental work

2.1. Chemicals

The chemicals which were used to synthesis 4A zeolite are hydrous sodium metasilicate ($Na_2SiO_3 \cdot 9H_2O$) supplied by Acros Organic, anhydrous sodium aluminate (Al_2O_3 55–56%wt) supplied by Riedel-deHaën, sodium hydroxide (NaOH pellets 99.9%wt) supplied by Fisher Scientific and deionized water. Metal ion solutions were prepared using nickel nitrate hexahydrate (99%wt) supplied by Merck and lead nitrate (99%wt) supplied by Chem-supply.

2.2. Preparation of 4A zeolite

Wide ranges of reaction compositions to prepare 4A zeolite have been presented in the literature. Different gel com-

position was chosen from the ranges given by [31], to study the effect of SiO_2/Al_2O_3, Na_2O/SiO_2, H_2O/Na_2O molar ratio on 4A zeolite formation. The procedures used to prepare 4A zeolite simulate to the preparation method used in [32,33]. Series of experiments was carried out to study the effect of crystallization temperature and crystallization time on the synthesized zeolite structure. Thus, the gel produced was crystallized in a Teflon-lined autoclave at different crystallization temperature 75, 100 and 125°C for different crystallization time 2.5, 4, 6, 24 h. The autoclaves were quenched at the end of crystallization time and the products were recovered, filtered and washed with deionized water until pH of the washing solution went below 9. After that, the products were dried at 50–80°C to be characterized by XRD, SEM, EDAX and Nitrogen adsorption/desorption isotherms.

2.3. Analytical techniques

XRD patterns of 4A zeolite samples were obtained using a Miniflex Rigaku X-ray analytical instrument of CuKα radiation source (λ = 1.5418 Å), voltage = 30 kV, current = 30 mA, scan speed = 3°min^{-1}, step size = 0.03, 2θ = 5–50° and total time ~ 20 min. The characterization of zeolite samples by both scanning electron microscopy (SEM) and energy dispersive analysis by X-ray (EDAX) was carried out via a model FEI Quanta 200. A sputter coater was used to coat the samples with gold to conduct the SEM imaging unlike the analysis by EDAX. The crystal size of samples was obtained via Image J software [34] for SEM images. Nitrogen adsorption/desorption isotherms were accomplished in this study using a micro metrics accelerated surface area and porosimetry (ASAP) 2010. Nitrogen gas at –200°C was used as an adsorbate.

2.4. Metal ions uptake

Removal of nickel ions (hydrated radius of 4.04 Å [35]) and lead ions (hydrated radius of 4.01 Å [35]) from water was studied using 4A zeolite samples. A simulated wastewater containing nickel ions and lead ions with a concentration of 200 ppm was prepared from dissolving nickel nitrate hexahydrate and lead nitrate in deionized water. 200 mg of the synthesized zeolite was added to 100 ml of the metal solutions [36]. A set of 125 ml tubes containing the contaminated water was shaken for 4 h at room temperature using a shaker at 250 rpm. The pH of solutions was measured initially and after 4 h. Zeolite suspension was removed by filtration before carrying out the analysis and the filtrate was taken to analysis. The concentration of ions in the solution was obtained using atomic absorption spectrophotometer (Perkin Elmer-5000). To identify the pH at which the metal hydroxides start precipitation, the pH of metal solutions was altered until the hydroxides started to precipitate. And this test was repeated for three times to achieve reliable results.

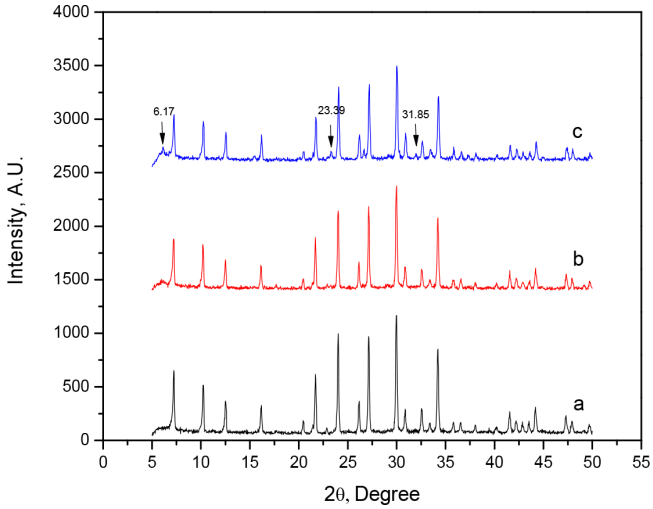

Fig. 1. XRD patterns of synthesis products crystallized for different SiO_2/Al_2O_3 mole ratio in reaction mixture: (a) 1, (b) 2, (c) 2.2 for Na_2O/SiO_2 = 3, H_2O/Na_2O = 35 and crystallization temperature 100°C for 4 h.

3. Results and discussion

3.1. SiO_2/Al_2O_3 molar ratio

The results of XRD analysis shown in Figs. 1 and 3 are for 4A zeolite samples prepared for various SiO_2/Al_2O_3 ratio at Na_2O/SiO_2 ratio of 3 and 2.5 respectively. XRD patterns showed crystallization of pure 4A zeolite phase when samples prepared with SiO_2/Al_2O_3 of 1 and 2. For samples prepared at SiO_2/Al_2O_3 of 2.2, the results showed appearing of peaks belongs to Faujasite (FAU) phase at 2θ around 6.17, 23.39 and 31.85. The appearance of FAU phase was obvious at 2θ around 6.17, 11.75, 15.53, 20.15, 23.39, 26.21, 31.85, 33.59 and 37.58 when the SiO_2/Al_2O_3 increased to 3 and Na_2O/SiO_2 was 2.5 (Fig. 3c). This can be attributed to the reduction of alkaline available in the reaction environ-

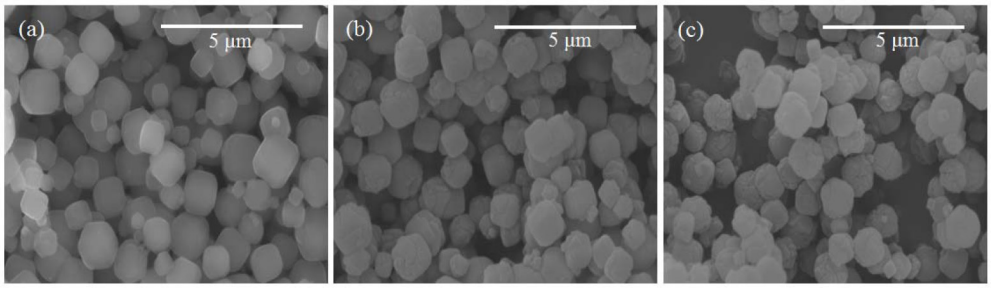

Fig. 2. SEM images of synthesis products crystallized for different SiO_2/Al_2O_3 mole ratio in reaction mixture: (a) 1, (b) 2, (c) 2.2 for Na_2O/SiO_2 = 3, H_2O/Na_2O = 35 and crystallization temperature 100°C for 4 h.

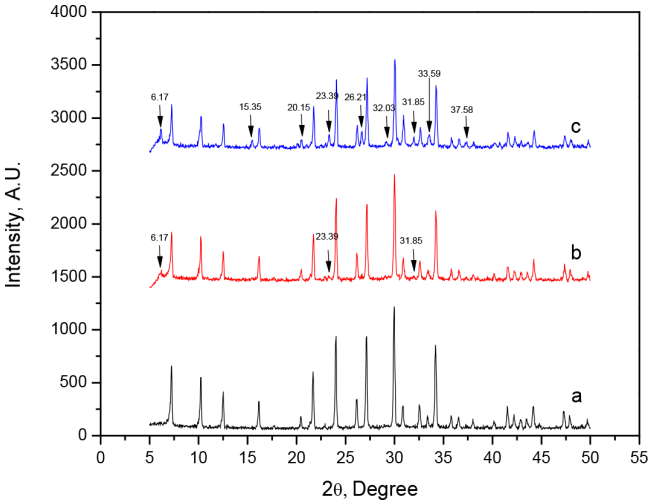

Fig. 3. XRD patterns of synthesis products crystallized for different SiO_2/Al_2O_3 mole ratio in reaction mixture: (a) 1, (b) 2, (c) 2.2 for Na_2O/SiO_2 = 2.5, H_2O/Na_2O = 35 and crystallization temperature 100°C for 4 h.

ment to provide mineralizing agent ($^-$OH). A mineralizer allows good silica and alumina species dissolving from their source to promote supersaturation state.

Figs. 2 and 4 show SEM images of 4A zeolite samples prepared for various SiO_2/Al_2O_3 ratio at Na_2O/SiO_2 ratio of 3 and 2.5 respectively. Well-defined cubic shaped with a smooth surface and curvy edge crystals were obtained at SiO_2/Al_2O_3 ratios of 1 and 2. SiO_2/Al_2O_3 ratio of 2.2 at Na_2O/SiO_2 ratio of 2.5 gave overlapped crystals with fragmented and coarse surfaces and edgeless morphology. Table 1 presents the particle size of the samples obtained using Image J software. Where, the crystal size of products decreased with increasing SiO_2/Al_2O_3 ratio. At the same SiO_2/Al_2O_3 molar ratio, when Na_2O/SiO_2 was 3 the crystal size is smaller than when it was 2.5. This is because high pH leads to increasing the supersaturation of silicate and aluminate and generation of a large number of nuclei, but the growth of these nuclei continues until exhausting of aluminum in the gel [19]. Also, EDAX results showing the quantitative analysis of the elements generating zeolite structure are presented in Table 1. The increasing in quantitative compositions of Si and Al is compatible with increasing SiO_2/Al_2O_3 ratio. Si/Al ratio increased with increasing SiO_2/Al_2O_3 ratio even when Na_2O/SiO_2 reduced from 3 to 2.5, however, the surface area reduced.

3.2. Na_2O/SiO_2 molar ratio

The XRD patterns shown in Figs. 5 and 7 are for 4A zeolite samples prepared at different Na_2O/SiO_2 and at SiO_2/Al_2O_3 of 1 and 2.2 respectively. Na_2O is generated from alkaline used for preparation, besides Na_2O present in alumina and silica sources. Alkalinity is a crucial parameter in the aluminosilica-based zeolite synthesis. Since, this important role of alkalinity arises from the vital role of OH- as a mineralizing agent. The mineralizing agent is a chemical species that forms a supersaturated solution from a gel, enables creation of a more stable solid phase from a less stable solid phase via crystallization process. Also, a mineralizing agent

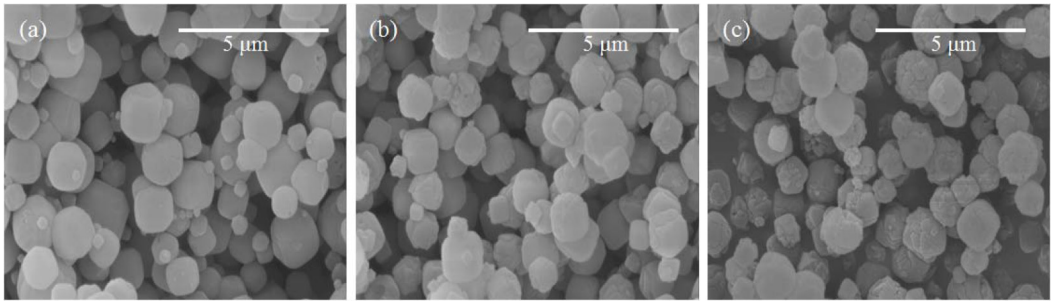

Fig. 4. SEM images of synthesis products crystallized for different SiO_2/Al_2O_3 mole ratio in reaction mixture: (a) 1, (b) 2, (c) 2.2 for Na_2O/SiO_2 = 2.5, H_2O/Na_2O = 35 and crystallization temperature 100°C for 4 h.

Table 1
Influence of SiO_2/Al_2O_3 mole ratio on the crystallization of zeolite phase. H_2O/Na_2O = 35, crystallization temperature = 100°C and crystallization time = 4 h

SiO_2/Al_2O_3	Na_2O/SiO_2	Elemental analysis, %				Si/Al	Crystal size (nm)	Surface area (m^2/g)	Nickel ion uptake%	Lead ion uptake%
		Al	Si	Na	O					
1	3	21.42	21.95	10.57	46.06	1	1040	356.432	78.46	99.86
2	3	19.84	22.31	11.30	46.55	1.1	975	333.894	80.68	99.78
2.2	3	20.34	23.28	12.81	43.57	1.15	974	226.994	72.39	99.72
1	2.5	21.15	21.44	11.09	46.32	1	1114	323.092	77.86	99.78
2	2.5	19.82	22.27	12.52	45.39	1.1	1180	298.202	75.98	99.64
2.2	2.5	19.69	22.62	12.55	45.34	1.15	1205	108.998	76.50	99.78

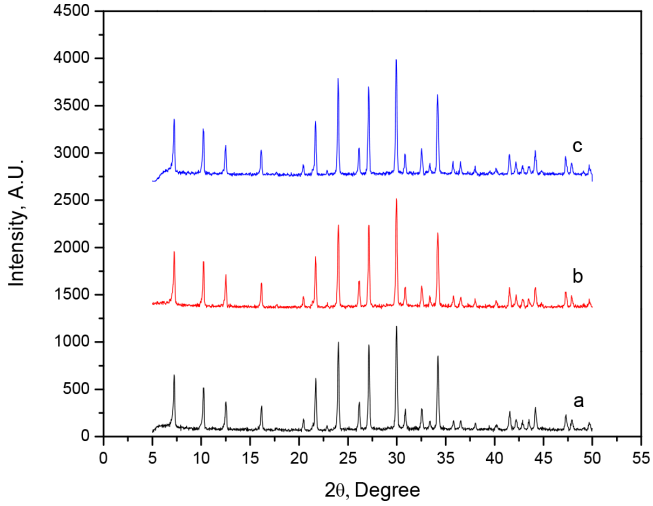

Fig. 5. XRD patterns of synthesis products crystallized for different Na_2O/SiO_2 mole ratio in reaction mixture: (a) 3, (b) 2.5, (c) 2.29 for SiO_2/Al_2O_3 = 1, H_2O/Na_2O = 35 and crystallization temperature 100°C for 4 h.

increases the overall solubility, reduces the induction and nucleation periods, increases the rate of conversion of all species in the solution mixture and accelerates crystal growth. Correspondingly, increasing the alkalinity reduces crystal size and minimizes the crystal size distribution [37].

Samples prepared at different chosen Na_2O/SiO_2 ratio and SiO_2/Al_2O_3 of 1 showed matched XRD patterns to LTA phase without irrelevant peaks. While for the samples prepared at Na_2O/SiO_2 of 2.29 and 2.5 and for SiO_2/Al_2O_3 of 2.2, peaks relevant to FUG phase appeared at 2θ around 6.17, 11.75, 15.53, 20.15, 23.39, 26.21, 31.85, 33.59 and 37.58. Peaks relevant to FAU phase obviously appeared for samples prepared with Na_2O/SiO_2 of 2.29, thus the product is a mixture of LTA and FAU phases. This can be attributed to the limited aluminum species dissolved in the reaction medium in conjunction with less Na^+ cations (structure stabilizing or directing agent) forming nucleation centers [38]. Nucleation centers for zeolite formation are generated through arranging of water molecules around the cations with subsequent displacement by silicate and aluminate species [38,39]. Varying the SiO_2/Al_2O_3 ratio affects the process of zeolite crystallization in term of the content and distribution of lattice Al, the kinetics of nucleation and crystallization, the morphology and crystal size and the crystallization material nature [38]. According to these results, mild and high alkalinity conditions are favorable for crystallization of zeolite 4A.

Fig. 6 shows SEM images of 4A zeolite samples prepared at different Na_2O/SiO_2 at SiO_2/Al_2O_3 of 1. Where the samples showed ordered cubic morphology with planar surfaces, non-sharp edges, and no change was observed in SEM by changing Na_2O/SiO_2 ratio. While, Fig. 8 shows SEM images of 4A zeolite samples prepared at different Na_2O/SiO_2 at SiO_2/Al_2O_3 of 2.2. These samples showed twined crystals with fragmented and coarse surfaces especially a sample prepared with Na_2O/SiO_2 of 2.29. Further reduction with Na_2O/SiO_2 ratio will result in an amorphous product, whereas sodalite forms together with 4A zeolite at extremely alkaline conditions as confirmed by results obtained by [19,20,40].

EDAX analysis giving the compositional information of the samples is shown in Table 2. Less alkalinity combined with higher SiO_2/Al_2O_3 ratio gave a mixture of LTA and FUG phases, thus higher Si/Al was obtained for the

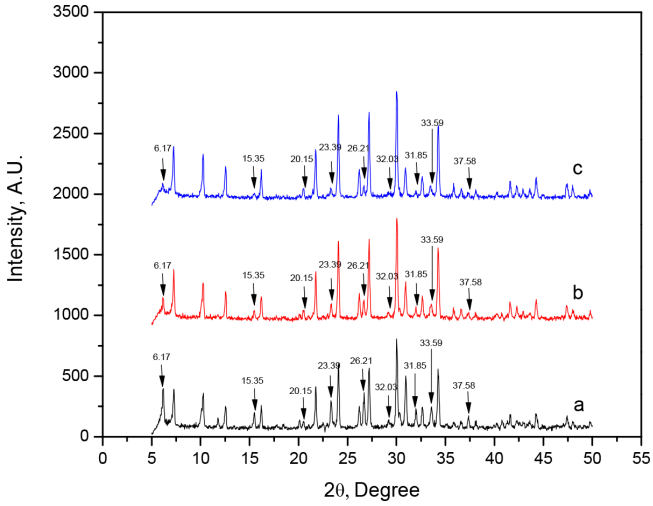

Fig. 7. XRD patterns of synthesis products crystallized for different Na_2O/SiO_2 mole ratio in reaction mixture: (a) 2.29, (b) 2.5, (c) 3 for SiO_2/Al_2O_3 = 2.2, H_2O/Na_2O = 35 and crystallization temperature 100°C for 4 h.

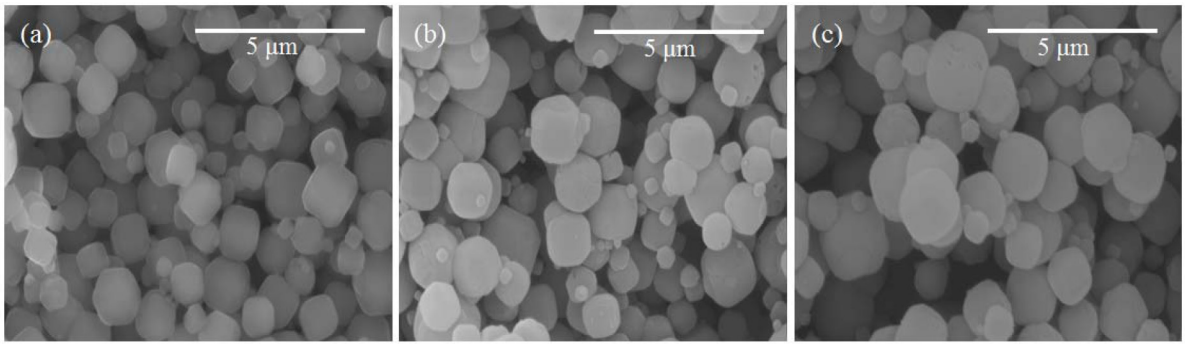

Fig. 6. SEM images of synthesis products crystallized for different Na_2O/SiO_2 mole ratio in reaction mixture: (a) 3, (b) 2.5, (c) 2.29 for SiO_2/Al_2O_3 = 1, H_2O/Na_2O = 35 and crystallization temperature 100°C for 4 h.

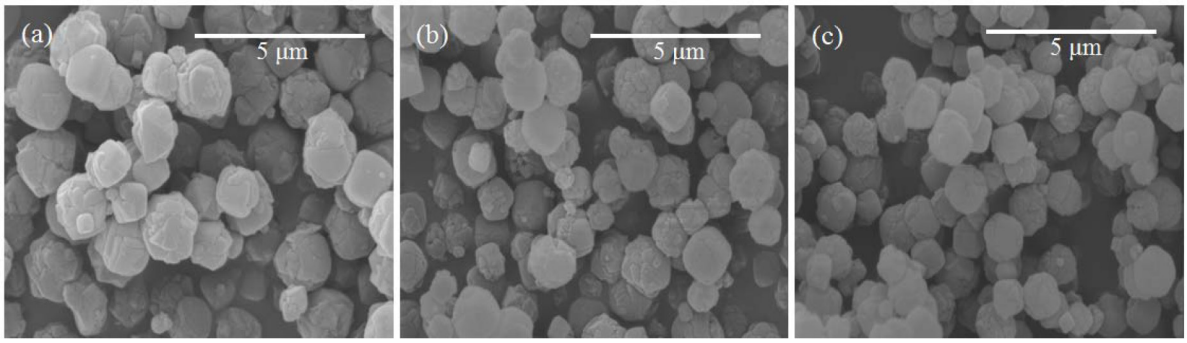

Fig. 8. SEM images of synthesis products crystallized for different Na_2O/SiO_2 mole ratio in reaction mixture: (a) 2.29, (b) 2.5, (c) 3 for SiO_2/Al_2O_3 = 2.2, H_2O/Na_2O = 35 and crystallization temperature 100°C for 4 h.

Table 2
Influence of Na_2O/SiO_2 mole ratio on the crystallization of zeolite phase. H_2O/Na_2O = 35, crystallization temperature = 100°C and crystallization time = 4 h

SiO_2/Al_2O_3	Na_2O/SiO_2	Elemental analysis, %				Si/Al	Crystal size (nm)	Surface area (m^2/g)	Nickel ion uptake%	Lead ion uptake%
		Al	Si	Na	O					
1	3	21.42	21.95	10.57	46.06	1	1040	356.432	78.46	99.86
1	2.5	21.15	21.44	11.09	46.32	1	1114	323.092	77.86	99.78
1	2.29	21.28	21.31	11.73	45.69	1	1263	220.837	77.78	99.32
2.2	3	20.34	23.28	12.81	43.57	1.15	974	326.994	72.39	99.72
2.2	2.5	19.69	22.62	12.55	45.34	1.15	1205	108.998	76.50	99.78
2.2	2.29	19.73	22.85	11.74	45.69	1.16	1262	178.116	–	–

samples prepared at different Na_2O/SiO_2 for SiO_2/Al_2O_3 of 2.2. While, Si/Al equal/close to 1 was obtained for other samples prepared to study the effect of Na_2O/SiO_2 molar ratio. Results presented in Table 2 show that the crystal size reduced by increasing Na_2O/SiO_2 because high alkalinity enhances nucleation rate on the expense of crystal growth which led to an increase in the zeolite surface area.

3.3. H_2O/Na_2O molar ratio

The amount of water added to the reaction mixture has a significant influence on the nucleation and crystallization of zeolite because it links to the alkalinity. Since higher H_2O/Na_2O ratio decreases the alkalinity, reduces the supersaturation and nucleation due to diluting the concentrations of silica and alumina species and ends with an amorphous final product. While lower H_2O/Na_2O ratio leads to crystallization of another phase in conjunction with crystallization of zeolite A. Fig. 9 shows the XRD patterns of 4A zeolite samples prepared for different H_2O/Na_2O ratio at SiO_2/Al_2O_3 of 2 and Na_2O/SiO_2 of 2. The XRD pattern of the 4A zeolite samples was identical to the standard pattern of LTA and no peaks relevant to undesired phases appeared in the XRD pattern of all samples. These results indicate that the chosen range of H_2O/Na_2O ratio (35–60) is likely favoured for crystallization pure phase of LTA.

Fig. 10 shows SEM images of the 4A zeolite samples prepared at different H_2O/Na_2O ratio. Increasing H_2O/Na_2O ratio to 45 and 60 resulted in crystals with a regular cubic morphology, planar surfaces with sharp and well-defined edges. Also, increasing H_2O/Na_2O ratio in the reaction mixture gave larger crystal size as revealed in Table 3, and larger surface area was obtained to the sample with H_2O/Na_2O ratio of 45. The quantification of the element by EDAX is shown in Table 3 confirmed XRD

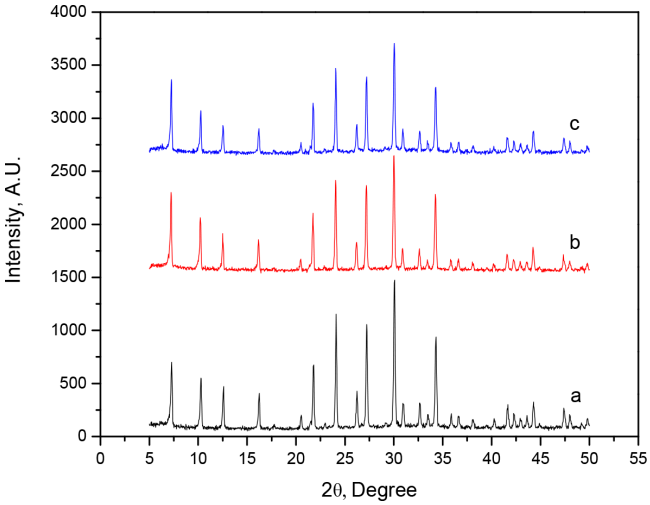

Fig. 9. XRD patterns of synthesis products crystallized for different H_2O/Na_2O mole ratio in reaction mixture: (a) 35, (b) 45, (c) 60 for SiO_2/Al_2O_3 = 2, Na_2O/SiO_2 = 2 and crystallization temperature 100°C for 4 h.

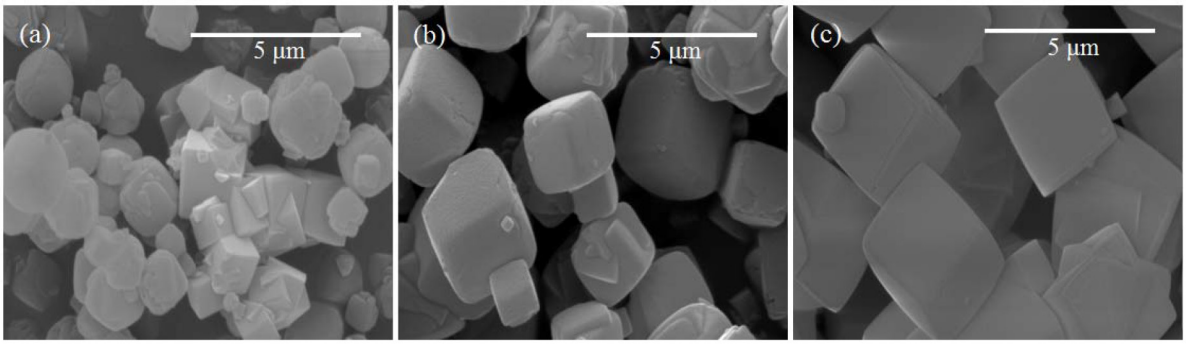

Fig. 10. SEM images of synthesis products crystallized for different H_2O/Na_2O mole ratio in reaction mixture: (a) 35, (b) 45, (c) 60 for SiO_2/Al_2O_3 = 2, Na_2O/SiO_2 = 2 and crystallization temperature 100°C for 4 h.

Table 3
Influence of H_2O/Na_2O mole ratio on the crystallization of zeolite phase. SiO_2/Al_2O_3 = 2, Na_2O/SiO_2 = 2, crystallization temperature = 100°C and crystallization time = 4 h

H_2O/Na_2O	Elemental analysis, %				Si/Al	Crystal size (nm)	Surface area (m^2/g)	Nickel ion uptake%	Lead ion uptake%
	Al	Si	Na	O					
35	20.59	23.47	10.88	45.05	1.1	1413	184.726	71.97	99.73
45	20.82	23.73	13.01	42.45	1.1	1916	224.647	65.80	99.64
60	19.84	22.72	12.27	45.16	1.1	2142	220.020	65.30	99.64

results which indicate crystallization of LTA phase having Si/Al ~ 1.

3.4. Crystallization temperature

Crystallization temperature significantly influences nucleation, crystal growth and size distribution of the crystals produced; thus a certain zeolite phase can be produced within a specified range of temperature. Higher crystallization temperature leads to larger crystal and higher growth rate because both nucleation rate and the crystal growth rate increase with increasing the temperature [39].

Variation of crystallization temperature on the zeolite crystal growth is shown in Figs. 11 and 12. An amorphous phase formed at 75°C, however, literature pointed out 70°C is not adequate for the formation of a crystalline phase [14,19] indicating the importance of crystallization time for the process. Higher crystallization temperature (beyond 120°C) leads to phase transformation to hydroxysodalite because of water evaporation during hydrothermal treatment causes increasing of sodium concentration in the liquid phase [41]. Raising crystallization temperature to 125°C showed no impure phases formed during crystallization. The sample crystallized at 125°C gave an identical XRD pattern to the sample crystallized at 100°C confirming the suitability of range 100–125°C for crystallization of 4A zeolite owning this gel formula 4 Na_2O: 2 SiO_2: 1 Al_2O_3: 180 H_2O. Crystals of cubic morphology well-defined edges formed for samples crystallized at 100°C and 125°C. However, the sample crystallized at 125°C was inter grown and twinned crystals. EDAX analysis presented in Table 4 shows that sample crystallized at 125°C possesses Si/Al of 1.17 which can be elucidated as that high temperature increases the alkalinity due to evaporation of water present in the reaction mixture, increase silicon solubility and thus Si/Al ratio. The crystal size increased with increasing crystallization temperature as presented in Table 4. Thus, the surface area reduced when increasing the crystallization to 125°C.

Rietveld refinement method combined with MAUD software, version 2.26 [42] was used to analyze anisotropic micro structure of zeolite samples prepared at different crystallization temperature. The results obtained from Rietveld refinement and Popa model approach used for the anisotropic micro structure analysis are shown in Table 5. The results obtained in this work are compati-

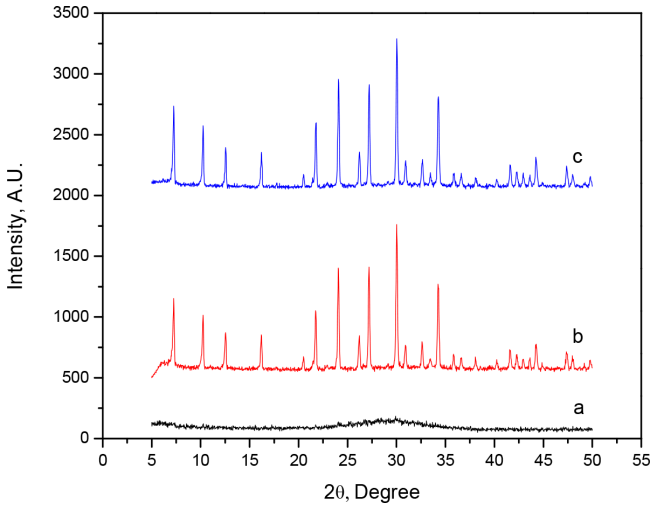

Fig. 11. XRD patterns of synthesis products crystallized for SiO_2/Al_2O_3 = 2, Na_2O/SiO_2 = 2, H_2O/Na_2O = 45, crystallization for 4 h and crystallization temperature of: (a) 75°C, (b) 100°C, (c) 125°C.

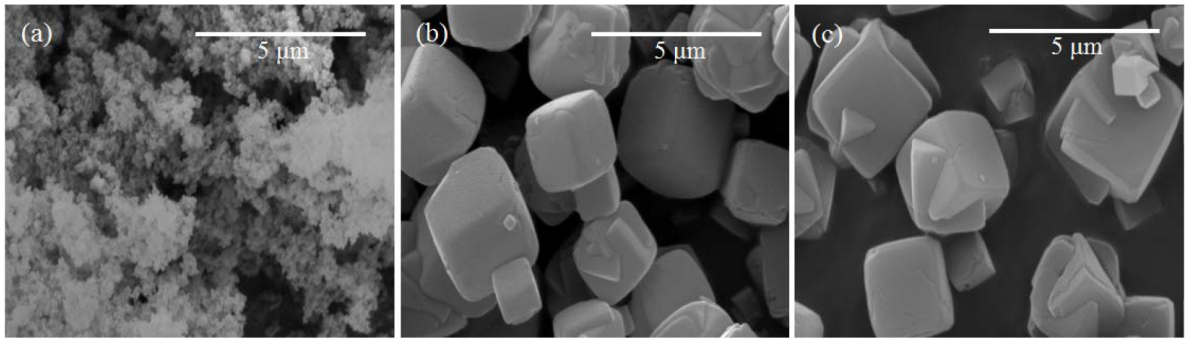

Fig. 12. SEM Images of synthesis products crystallized for SiO_2/Al_2O_3 = 2, Na_2O/SiO_2 = 2, H_2O/Na_2O = 45, crystallization for 4 h and crystallization temperature of: (a) 75°C, (b) 100°C, (c) 125°C.

Table 4
Influence of crystallization temperature on the crystallization of zeolite phase. SiO_2/Al_2O_3 = 2, Na_2O/SiO_2 = 2, H_2O/Na_2O = 45 and crystallization time = 4 h

Crystallization temperature, °C	Elemental analysis, %				Si/Al	Crystal size (nm)	Surface area (m^2/g)	Nickel ion uptake%	Lead ion uptake%
	Al	Si	Na	O					
75	19.78	23.56	11.49	45.17	–	Amorphous	4.654	–	–
100	20.82	23.73	13.01	42.45	1.1	1916	224.647	65.80	99.64
125	19.62	22.97	12.81	44	1.17	2439	210.994	63.68	99.78

Table 5
Rietveld refinement and Popa model approach parameters

Refinement results	Crystallization temperature, °C		
	75	100	125
Cell length, Å	24.725	24.613	24.612
Density, g/cm^3	1.9916	2.0188	2.0193
Popa model micro structure micro strain value	0.04727	0.0006517	–0.001133
Error%	14.64E-4	1.0848E-4	1.959E-4

ble with those obtained in the previous work [33]. Where for samples crystallized at 100°C and 125°C, the micro strain values are far enough from the value of sample crystallized at 75°C. The variance in micro strain value of sample crystallized at 75°C with high error percent is due to the formation of an amorphous consistency and generation of micro pores not yet accomplished at this temperature.

3.5. Crystallization time

The morphology and crystal size of the final product is significantly influenced by crystallization time. The XRD patterns of samples crystallized from 4 Na_2O: 2 SiO_2: 1 Al_2O_3: 180 H_2O at different crystallization time are shown in Fig. 13. Crystallization for 2.5 h gave an amorphous phase and increasing time to 4 and 6 h increases the crystallinity of the synthesized products. When the crystallization was extended to 24 h, the peaks did not intensify further but they still refer to 4A zeolite. XRD results confirmed the results obtained by EDAX analysis shown in Table 6 which display Si/Al ratio of the samples and it was around 1 for samples crystallized for more than 2.5 h.

The SEM image in Fig. 14 shows formation of few crystals in the final product in conjunction with the formation of the amorphous phase when the crystallization process was conducted for 2.5 h. When crystallization time was prolonged to 6 h, large cubic crystals with planer surfaces and well-defined edges were obtained. Extending crystallization time to 24 h resulted in more twinned and inter grown crystals. Table 6 shows that the crystal size of prod-

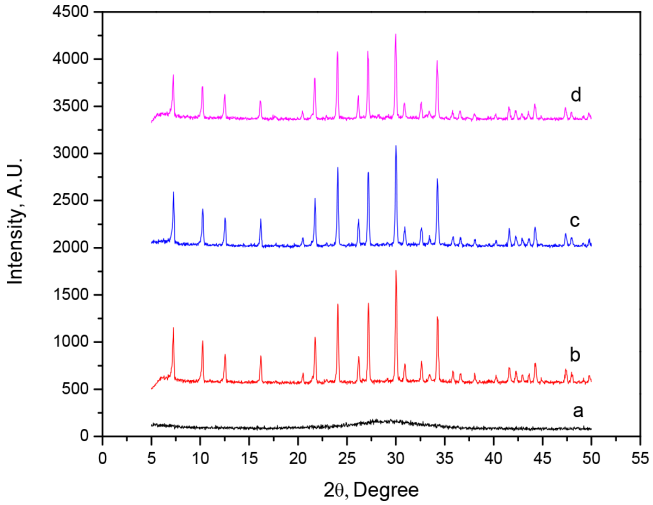

Fig. 13. XRD patterns of synthesis products crystallized for SiO_2/Al_2O_3 = 2, Na_2O/SiO_2 = 2, H_2O/Na_2O = 45, crystallization temperature of 100°C and crystallization time of: (a) 2 h, (b) 4 h, (c) 6 h, (d) 24 h.

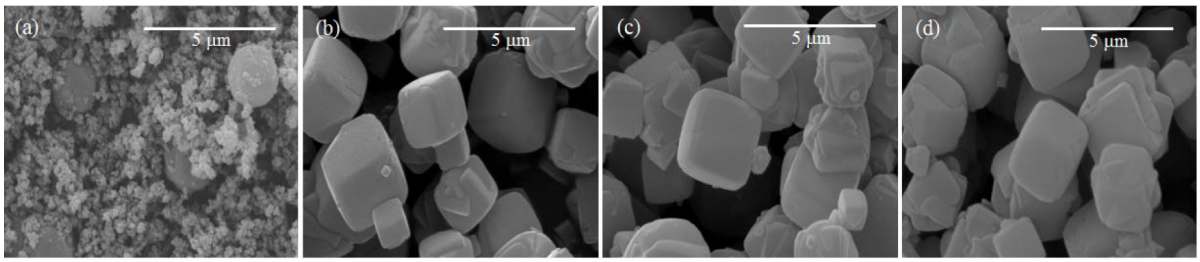

Fig. 14. SEM images of synthesis products crystallized for SiO_2/Al_2O_3 = 2, Na_2O/SiO_2 = 2, H_2O/Na_2O = 45, crystallization temperature of 100°C and crystallization time of: (a) 2 h, (b) 4 h, (c) 6 h, (d) 24 h.

Table 6
Influence of crystallization time on the crystallization of zeolite A phase. SiO_2/Al_2O_3 = 2, Na_2O/SiO_2 = 2, H_2O/Na_2O = 45 and crystallization temperature = 100°C

Crystallization time, h	Elemental analysis, %				Si/Al	Crystal size (nm)	Surface area (m^2/g)	Nickel ion uptake%	Lead ion uptake%
	Al	Si	Na	O					
2:30	20.90	25.22	11.60	42.29	–	Amorphous	4.825	–	–
4	20.82	23.73	13.01	42.45	1.1	1916	224.647	65.80	99.64
6	21	23.72	13.39	42.04	1.1	1262	298.292	63.68	99.73
24	20.26	23.08	12.56	44.09	1.1	897	260.82	61.37	99.78

uct became larger by increasing crystallization time due to increasing the rate of crystal growth.

N_2 adsorption/desorption isotherm results presented in Tables 1–6 (except Table 5) show the BET surface area of 4A zeolite samples. Increasing the H_2O/Na_2O ratio and crystallization temperature led to reducing the micro porous surface area of the zeolite samples. This can be attributed to increasing zeolite crystal size of these samples. However, the amorphous samples gave too small surface area due to that the formation of micro pores did not accomplish yet. Other zeolite samples possessing higher BET surface areas demonstrated eminent ability to remove the metal ions because higher surface area implies higher accessibility to the ion-exchange sites in the zeolite.

3.6. Metal ions uptake

The results of nickel and lead ions removal from water are shown in Tables 1–6 (except Table 5). All 4A zeolite samples favored lead ion than nickel ion. The uptake removal of lead ion reached 99.9%, however for nickel ion did not exceed 80.6%. The difference between hydrous radiuses of ions may elucidate the difference in the ions uptake on zeolite 4A which has a pore size of 4 Å. The size of the hydrated ion is one of the factors that dominate the uptake of ions by zeolite 4A [11,43]. When the hydrous radius of ion is greater than the pore size of zeolite 4A, the ions may be expelled. While in the case of the solvated ions, some of the hydration waters must be detached to enable ions to enter zeolite pores [11].

Obtaining high readings of solution pH at the end of the removal process corroborates occurring of the ion-exchange process. The pH of lead solutions eventually increased to 9.8 when it had started at 5.35. While, the pH of nickel solutions had started at 6.33 and ended with 7.7. Generally, the structure of low Si/Al zeolite is weakly acidic, accordingly, sodium form zeolites are selective for hydrogen ($RNa + H_2O \Leftrightarrow RH + Na^+ + OH^-$). pH raises when these zeolites are equilibrated with a relatively dilute electrolyte solution. When pH increases, deprotonation of functional groups occurs and zeolites behave as negatively charged formed to attract heavy metals. This leads to precipitation of metal hydroxide due to decreasing the solubility of metals [11,44]. Karimi [45] reported that the minimum solubility of lead hydroxide is at pH range of 9–11 and for nickel hydroxide is at pH range of 8–11.6.

High pH resulting from the uptake of lead ions gave rise to formation and precipitation of lead hydroxide which started at pH around 6.2. The solubility of lead hydroxide decreases with continuous increase in pH. Eventually, it can be said that the comprehensive removal of lead ions arises from ion-exchange process accompanied with precipitation process. However, removal of nickel ions can only be attributed to the ion-exchange process because formation and precipitation of nickel hydroxide start at pH above 8. Same results were obtained when other types of zeolites were used such as clinoptilolite [43,46,47]. So far, various phases of zeolites rather than LTA have been successfully examined to remove other heavy metals and they can be a good choice to remove both lead and nickel ions, such as zeolite X and zeolite Y [48,49].

4. Conclusions

The experimental study described in this research presents the significant effect of several synthesis parameters on the crystallinity, crystal size and morphology of 4A zeolite. High SiO_2/Al_2O_3 and Na_2O/SiO_2 molar ratio favored formation of Faujasite phase. The formation of a well-defined cubic end product is favoured within a spe-

cific range of H_2O/Na_2O molar ratio. Also, extending the crystallization time to 24 h favored formation of twinned and inter grown crystals. For a chosen gel formula, the synthesized product was amorphous including a few crystals of 4A zeolite when the crystallization temperature was 75°C. The Rietveld refinement analysis revealed that the micro strain values for an amorphous sample significantly vary from those values for the well-crystallized samples which were prepared to study the effect of crystallization temperature. The removal of lead ions from aqueous solution was favored than nickel ion for all 4A zeolite samples. Since the higher percentage removal for nickel was 80.68% compared to lead ions was 99.86%. Unlike removal of nickel ion, the removal of lead ions is a combination of ion-exchange and precipitation processes. Eventually, safe and successful treatment of wastewater contaminated with heavy metals can be attained using inexpensive ion-exchanger which can be conventionally prepared during a short time.

Acknowledgment

The authors would like to thank the Higher Committee for Education Development in Iraq for financially supporting Sama M. Al-Jubouri to conduct this work on the University of Manchester labs. Also, the authors would like to specifically thank Prof. Dr. Stuart M. Holmes and Dr. Patrick Hill.

References

[1] H.S. Ibrahim, T.S. Jamil, E.Z. Hegazy, Application of zeolite prepared from Egyptian kaolin for the removal of heavy metals: II. Isotherm models, J. Hazard. Mater., 182 (2010) 842–847.
[2] M. Ghaedi, S. Hajati, F. Karimi, B. Barazesh, G. Ghezelbash, Equilibrium, kinetic and isotherm of some metal ion biosorption, J. Ind. Eng. Chem., 19 (2013) 987–992.
[3] W. Qiu, Y. Zheng, Removal of lead, copper, nickel, cobalt, and zinc from water by a cancrinite-type zeolite synthesized from fly ash, Chem. Eng. J., 145 (2009) 483–488.
[4] H. Karadede-Akin, E. Ünlü, Heavy metal concentrations in water, sediment, fish and some benthic organisms from Tigris River, Turkey, Environ. Monit. Assess., 131 (2007) 323–337.
[5] T.S. Jamil, H.S. Ibrahim, I.H. Abd El-Maksoud, S.T. El-Wakeel, Application of zeolite prepared from Egyptian kaolin for removal of heavy metals: I. Optimum conditions, Desalination, 258 (2010) 34–40.
[6] B. Alyüz, S. Veli, Kinetics and equilibrium studies for the removal of nickel and zinc from aqueous solutions by ion exchange resins, J. Hazard. Mater., 167 (2009) 482–488.
[7] S.M. Kanawade, R.W. Gaikwad, Lead ion removal from industrial effluent by using biomaterials as an adsorbent, Int. J. Chem. Eng. Appl., 2 (2011) 196–198.
[8] Y.F. Tao, Y. Qiu, S.Y. Fang, Z.Y. Liu, Y. Wang, J.H. Zhu, Trapping the lead ion in multi-components aqueous solution by natural clinoptilolite, J. Hazard. Mater., 180 (2010) 282–288.
[9] World Health Organization (WHO), Guidelines for Drinking-water Quality, World Health, 1 (2011) 104–108.
[10] EU-legislation doc., Transposition of the " Council Directive 98/83/EC of 3 Nov 1998 on quality of water intended for human consumption " into the national laws in the EU associated countries, 1999. http://www.szu.cz/uploads/documents/chzp/voda/pdf/proc99.pdf.
[11] K.S. Hui, C.Y.H. Chao, S.C. Kot, Removal of mixed heavy metal ions in wastewater by zeolite 4A and residual products from recycled coal fly ash, J. Hazard. Mater., 127 (2005) 89–101.
[12] A. Nilchi, R. Saberi, M. Moradi, H. Azizpour, R. Zarghami, Adsorption of cesium on copper hexacyanoferrate-PAN composite ion exchanger from aqueous solution, Chem. Eng. J., 172 (2011) 572–580.
[13] A.A. Mohammed, Biosorption of lead, cadmium, and zinc onto sunflower shell: equilibrium, kinetic, and thermodynamic studies, Iraqi J. Chem. Pet. Eng., 16 (2015) 91–105.
[14] X.D. Liu, Y.P. Wang, X.M. Cui, Y. He, J. Mao, Influence of synthesis parameters on NaA zeolite crystals, Powder Technol., 243 (2013) 184–193.
[15] S.M. Auerbach, K.A. Carrado, P.K. Dutta, P.K. Payra, Pramatha and Dutta, Handbook of Zeolite Science and Technology, Handb. Zeolite Sci. Technol., (2003) 1–19.
[16] D.A.D.H.-D. Rio, S.M. Al-Jubouri, S.M. Holmes, Hierarchical porous structured zeolite composite for removal of ionic contaminants from waste streams, Chim. Oggi - Chem. Today, 35 (2017) 26–29.
[17] L.E. Smart, E.A. Moore, Solid state chemistry: An Introduction, Third Edit, Taylor & Francis Group, Boca Raton London New York Singapore, 2005.
[18] R.F. de Farias, Interface Science and Technology, 17 (2009) 109–112.
[19] E.B.G. Johnson, S.E. Arshad, Hydrothermally synthesized zeolites based on kaolinite: A review, Appl. Clay Sci., 97–98 (2014) 215–221.
[20] X. Zhang, D. Tong, W. Jia, D. Tang, X. Li, R. Yang, Studies on room-temperature synthesis of zeolite NaA, Mater. Res. Bull., 52 (2014) 96–102.
[21] X. Zhang, D. Tang, G. Jiang, Synthesis of zeolite NaA at room temperature: The effect of synthesis parameters on crystal size and its size distribution, Adv. Powder Technol., 24 (2013) 689–696.
[22] C.A. Ríos, C.D. Williams, O.M. Castellanos, Crystallization of low silica Na-A and Na-X zeolites from transformation of kaolin and obsidian by alkaline fusion., Cristal. Zeolitas Na-A y Na-X Bajas En Sílice a Partir La Transform. Caolín y Obs. Por Fusión Alcalina. 14 (2012) 125–137.
[23] R.M. Mohamed, A.a. Ismail, G. Kini, I.a. Ibrahim, B. Koopman, Synthesis of highly ordered cubic zeolite A and its ion-exchange behavior, Colloids Surfaces A Physicochem. Eng. Asp., 348 (2009) 87–92.
[24] A.R. Loiola, J.C.R.A. Andrade, J.M. Sasaki, L.R.D. da Silva, Structural analysis of zeolite NaA synthesized by a cost-effective hydrothermal method using kaolin and its use as water softener, J. Colloid Interface Sci., 367 (2012) 502–508.
[25] G. Tutuncu, Analysis and interpretation of diffraction data from complex, anisotropic materials, Iowa State University, 2010.
[26] L. Lutterotti, S. Matthies, H.R. Wenk, A.S. Schultz, J.W. Richardson, Combined texture and structure analysis of deformed limestone from time-of-flight neutron diffraction spectra, J. Appl. Phys., 81 (1997) 594–600.
[27] L. Lutterotti, R. Vasin, H.R. Wenk, Rietveld texture analysis from synchrotron diffraction images, I. Calibration and basic analysis, Powder Diffr., 29 (2014) 76–84.
[28] N.C. Popa, The (hkl) Dependence of diffraction-line broadening caused by strain and size for all laue groups in rietveld refinement, J. Appl. Crystallogr., 31 (1998) 176–180.
[29] A. Leineweber, Understanding anisotropic micro strain broadening in Rietveld refinement, Z. Krist., 226 (2011) 905–923.
[30] A. Palčić, B. Subotić, V. Valtchev, J. Bronić, Nucleation and crystal growth of zeolite A synthesised from hydro gels of different density, Cryst. Eng. Comm., 15 (2013) 5784.
[31] E.C. Soule, N. Falls, US2882243, (1943) 19–22.
[32] H. Robson, Verified synthesis of zeolitic materials, Elsevier Science, 2001.
[33] S.M. Al-Jubouri, B.I. Waisi, S.M. Holmes, Rietveld texture refinement analysis of LTA zeolite from X-Ray diffraction data, J. Eng. Sci. Technol., 13 (2018) 4066–4077.
[34] Image processing and analysis in Java, Image J. Software, Https://Imagej.Nih.Gov/Ij/Index.Html. (2018).
[35] R. Nightingale, Phenomenological theory of ion solvation. effective radii of hydrated ions, J. Phys. Chem., 63 (1959) 1381–

1387.
[36] S.M. Al-Jubouri, N.A. Curry, S.M. Holmes, Hierarchical porous structured zeolite composite for removal of ionic contaminants from waste streams and effective encapsulation of hazardous waste, J. Hazard. Mater., 320 (2016) 241–251.
[37] J.W. L. Puppe, Catalysis and Zeolites, First, Springer-Verlag Berlin Heidelberg GmbH, Germany, 1999.
[38] K. Byrappa, M. Yoshimura, Handbook of hydrothermal technology, 2nd ed., Elsevier, Amsterdam - Oxford - New York - Tokyo, 2013.
[39] J. Cejka, H. Van Bekkum, A. Corma, F. Schüth, Introduction to zeolite science and practice, Elsevier BV Amsterdam, Neth, 2007.
[40] C.A.R. Reyes, C.D. Williams, O.M.C. Alarcón, Synthesis of zeolite LTA from thermally treated kaolinite | Síntesis de zeolita LTA a partir de caolinita tratada térmicamente, Rev. Fac. Ing., (2010) 30–41.
[41] A.a. Ismail, R.M. Mohamed, I.a. Ibrahim, G. Kini, B. Koopman, Synthesis, optimization and characterization of zeolite A and its ion-exchange properties, Colloids Surfaces, A Physicochem. Eng. Asp., 366 (2010) 80–87.
[42] L. Lutterotti, Total pattern fitting for the combined size–strain–stress–texture determination in thin film diffraction, Nucl. Instruments Methods Phys. Res. Sect. B Beam Interact. with Mater. Atoms, 268 (2010) 334–340.
[43] S.M. Shaheen, A.S. Derbalah, F.S. Moghanm, Removal of heavy metals from aqueous solution by zeolite in competitive sorption system, Int. J. Environ. Sci. Dev., 3 (2012) 362–367.
[44] M.A. Wassel, H.A. Shehata, H.F. Youssef, A.S. Elzaref, A. Fahmy, Nickel ions adsorption by prepared zeolite-A: Examination of process parameters, Kinet. Isotherm., 3 (2016) 422–429.
[45] H. Karimi, Effect of pH and initial pb(II) concentration on the lead removal efficiency from Industrial wastewater using $Ca(OH)_2$, Int. J. Water Wastewater Treat., 3 (2017). doi:10.16966/2381-5299.139.
[46] A.L. Ciosek, G.K. Luk, Kinetic modelling of the removal of multiple heavy metallic ions from mine waste by natural zeolite sorption, Water (Switzerland), 9 (2017). doi: 10.3390/w9070482.
[47] A. Zendelska, M. Golomeova, K. Lisichkov, S. Kuvendziev, Characterization and application of clinoptilolite for removal of heavy metal ions from water resources, Geol. Maced., 32 (2018) 21–32.
[48] J.S. Kim, M.A. Keane, Ion exchange of divalent cobalt and iron with Na–Y zeolite: binary and ternary exchange equilibria, J. Colloid Interface Sci., 232 (2000) 126–132.
[49] S.M. Al-Jubouri, S.M. Holmes, Hierarchically porous zeolite X composites for manganese ion-exchange and solidification: Equilibrium isotherms, kinetic and thermodynamic studies, Chem. Eng. J., 308 (2017) 476–491.